BMC Pediatrics

CASE REPORT

Open Access

Long read Nanopore sequencing identifies precise breakpoints of a *de novo* paracentric inversion that disrupt the MEIS2 gene in a Chinese girl with syndromic developmental delay

Jianxin Tan[1†], Mingtao Huang[1†], Xiuqing Ji[1], An Liu[1], Fengchang Qiao[1], Cuiping Zhang[1], Lulu Meng[1], Yan Wang[1], Zhengfeng Xu[1*] and Ping Hu[1*]

Abstract

Background Chromosomal inversions are underappreciated causes of rare diseases given their detection, resolution, and clinical interpretation remain challenging. Heterozygous mutations in the *MEIS2* gene cause an autosomal dominant syndrome characterized by intellectual disability, cleft palate, congenital heart defect, and facial dysmorphism at variable severity and penetrance.

Case presentation Herein, we report a Chinese girl with intellectual disability, developmental delay, and congenital heart defect, in whom G-banded karyotype analysis identified a *de novo* paracentric inversion 46,XX, inv(15)(q15q26.1) and other conventional approaches including chromosomal microarray analysis and whole exome sequencing were failed to detect any pathologic variants that can explain the phenotypes of the proband. Subsequently, long-read Nanopore sequencing was directly conducted and defined the breakpoint position of the inversion, disrupting the *MEIS2* gene at intron 8. These breakpoints were also confirmed by Sanger sequencing.

Conclusions In conclusion, we report the first chromosomal inversion disrupting the *MEIS2* gene, which was fine-mapped by long read Nanopore sequencing. Our data not only expand the clinical spectrum of MEIS2-caused syndromic developmental delay, but also illustrate the value of long-read sequencing in elucidating the precise genetic etiology of patients with relatively nonspecific clinical findings and chromosomal inversion that are beyond the resolution of conventional approaches.

Keywords Long read sequencing, MEIS2, Paracentric inversion, Syndromic developmental delay

†Jianxin Tan and Mingtao Huang contributed equally to this work.

*Correspondence:
Zhengfeng Xu
zhengfengxu@njmu.edu.cn

Ping Hu
njfybjyhuping@163.com
[1]Department of Prenatal Diagnosis, Women's Hospital of Nanjing Medical University, Nanjing Women and Children's Healthcare Hospital, 123 Tianfei Alley, Nanjing 210004, People's Republic of China

Background

Chromosomal inversions are a unique class of structural variation (SV) that occurs as a result of intrachromosomal breakage and reunion of segments in the opposite orientation. Apart from an increased risk for miscarriages, inversions are traditionally considered as genomic polymorphisms without apparent phenotypic consequences because inversion carriers have no overall gain or loss of genetic material [1]. However, emerging evidence indicates that SVs, including inversions, are underappreciated causes of rare diseases given their detection, resolution, and clinical interpretation remain challenging [2]. Therefore, identification of pathogenic SVs will result in an increased diagnostic rate of rare diseases, thereby improving genetic counseling, management, and prognosis of these conditions.

Traditionally, inversions were detected by conventional karyotype analysis, but this approach has a limited resolution of approximately 5–10 Mb [3]. Routine molecular approaches including chromosomal microarray analysis (CMA) and exome sequencing (ES) cannot detect most inversions because they are copy-number neutral and their breakpoints usually located in non-coding regions [4]. The emergence of whole genome sequencing (WGS) has the potential to detect inversion events, but it suffers from relatively high false positive and false negative rates [5]. More recently, the long-read sequencing technologies, such as Oxford Nanopore, Pacific Biosciences (PacBio) and optical genome mapping have allowed a further increase in the sensitivity of inversion detection [6].

Herein, we described a Chinese girl with syndromic developmental delay and a paracentric inversion. To experimentally dissect the genomic architecture of this inversion, and to explore whether genes involved in the inversion contributed to the clinical phenotype of this patient, multiple approaches including karyotype analysis (G-banding), nanopore-based long-read sequencing, and Sanger sequencing were used in this study. The convergence of experimental approaches enabled the characterization of this inversion to the DNA base-pair level of resolution, disrupting the coding sequencing of the Meis homeobox 2 (*MEIS2*) gene and explaining the clinical phenotype in this patient.

Case presentation

The proband (Fig. 1A), a 5-year-old girl, was born to healthy nonconsanguineous Chinese parents at 36 weeks of gestation *via* cesarean operation because of oligohydramnios and abnormal fetal heart rate. Her birth length is 41 cm (-5.1 SD), and her birth weight is 1.95 kg (-3.5 SD). She was transferred to the neonatal intensive care unit because of premature birth and underwent an operation for ventricular septal defect closure, patent ductus arteriosus and tricuspid annuloplasty at 3 months after birth. On examination at 4 years and 3 months of age, her weight was 10 kg (-3.2 SD), her height was 95 cm (-2.5 SD), and her occipitofrontal head circumference 47 cm (-2.0 SD). She exhibited a moderate facial dysmorphism with short stature, broad forehead, arched eyebrows, sparse eyebrows deeply set eyes, and large and low-set ears (Fig. 1B). She had delayed motor development, intellectual disability, learning difficulties with poor speech and irrelevant answers. Additional biochemical assays and neonatal genetic metabolic disease screening were normal.

After consultation with a clinical geneticist, conventional chromosomal G-banding karyotype analysis and chromosomal microarray analysis (CMA) were performed. As a result, karyotype analysis identified a balanced paracentric inversion, 46, XX, inv (15)(q15q26.1) in the proband (Fig. 1C), and no gain or loss of genetic material was resolved by using a high-resolution 750 K array (data not shown). Her parents showed normal CMA and karyotype results. Next, trio-whole exome sequencing (trio-WES) was carried out, but no pathogenetic/likely pathogenic single-nucleotide variant (SNV) or small insertion/deletion that can explain the phenotypes of the proband were identified. Thus, this proband remained genetically undiagnosed.

In order to explore the potential genetic cause, a long-read Nanopore whole genome sequencing was performed on this proband. Genomic DNA was extracted from peripheral blood samples using a QIAGEN genomic DNA extraction kit (Cat#13323, QIAGEN, Hilden, Germany) and quantified using a Qubit 3.0 Fluorometer (Invitrogen, Carlsbad, CA, USA). Subsequently, long DNA fragments were size selected using the BluePippin system (Sage Science, Beverly, MA, USA). Whole-genome libraries were prepared using the Ligation Sequencing kit 1D (SQK-LSK109, Oxford Nanopore Technologies, ONT, Oxford, UK) in accordance with the manufacturer's instructions. The libraries were then loaded into R9.4(1D) flow cells and sequenced on the PromethION sequencer (ONT). Then Guppy (version: 2.0.8) was used to perform base-calling on fast5 files to generate FASTQ format files. Raw data collected as FAST5 files were converted to FASTQ format using guppy 4.5.3 (ONTs). Base-called data passing quality control (quality score≥9) was aligned to the hg19 human reference genome using Minimap2 (version 2.17) (github.com/lh3/minimap2). SVs were called with Sniffles (version 1.0.11) (github.com/fritzsedlazeck/Sniffles), and the major types of SVs included deletion, insertion, duplication, inversion, and translocation. Further annotation of SVs was carried out using ANNOVAR (github.com/WGLab/doc-ANNOVAR), combining public databases such as Chinese SVs database, 1,000 Genome Phase 3 DGV gold standard CNV

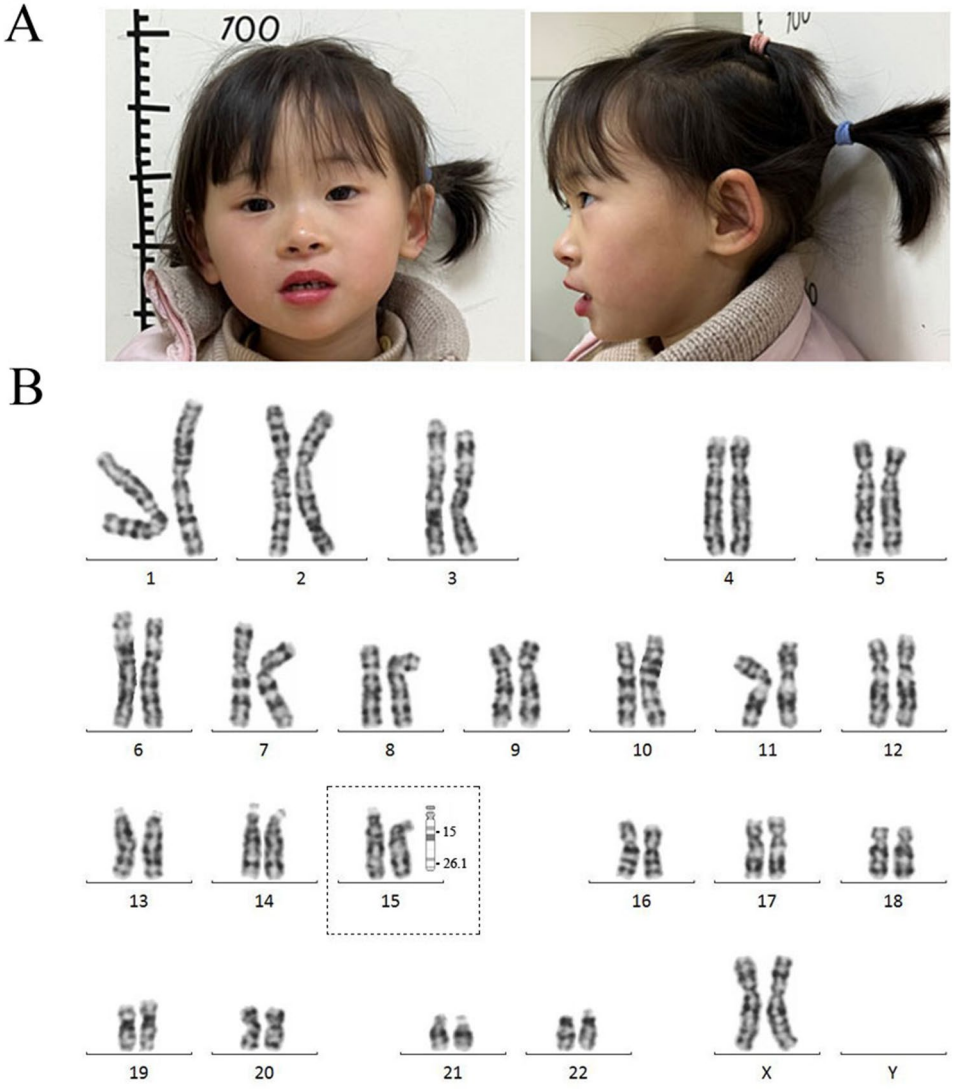

Fig. 1 Clinical characteristics of the proband. (**A**) Photograph of the proband. (**B**) Karyotype analysis revealed a *de novo* paracentric inversion 46,XX, inv (15)(q15q26.1) in the proband

dbVar nstd37 and DECIPHER. As a result, an average sequence depth of 15× was achieved. A total of 38,184 SVs including 6,439 translocations and 1,542 inversions was identified. After filtered out nonpathogenic SVs with the 405 unrelated Chinese individual database, a total of 1,494 SVs including 28 inversions was obtained (Fig. 2A). These 1,494 SVs were annotated with AnnotSV 3.0.9 and filtered out with OMIM database, and a total of 44 SVs were obtained, including 12 deletions, 18 insertions, 5 inversion and 9 translocations (Fig. 2B). Among these 44 SVs, 50 breakpoints affecting 45 genes were further analyzed to confirm whether the clinical phenotypes caused by these genes were consistent with those of the proband. We found that 12 genes were associated with delayed motor development and mild intellectual disability and 4 genes were associated with in heart disease. Then, we used the Integrative Genomics Viewer (IGV) program to eliminate probable false-positive SVs, and 38 genes were excluded. Finally, 7 genes were identified, including *SAR1B* (OMIM 246700), *MEIS2* (OMIM 600987), *PNPT1* (OMIM 608703), *SDHC* (OMIM 605373), *LIPC* (OMIM 614025), *TMEM38B* (OMIM 615066) and *GRID2* (OMIM 616204). Based on the long-read sequencing, the paracentric inversion, 46, XX, inv (15)(q15q26.1) identified by G-banding karyotype analysis was confirmed as 46,XX, inv (15)(q14q25.2). The inversion breakpoints were defined by chimeric reads mapping to 15q14 and 15 q25.2, corresponding to position chr15: 37,279,864 and chr15: 91,109,800 (hg19), respectively. This variant was finally characterized as follows: NC_000015.10:g.[37279864_37279910del;37279911_91109796inv;91109797_91109800del]. The upstream junction disrupted

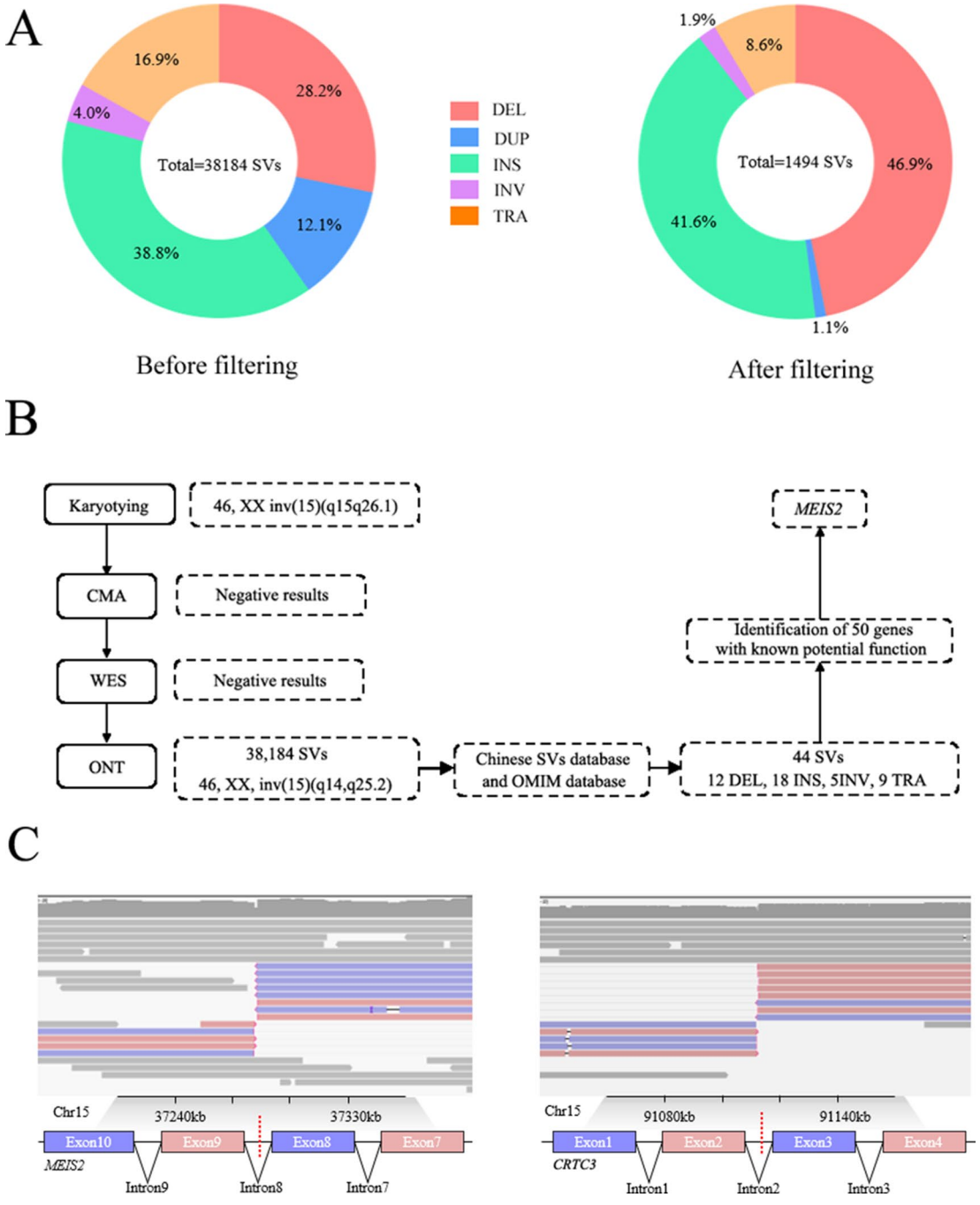

Fig. 2 Analysis of the proband by nanopore-based long-read sequencing. (**A**) SVs identified by nanopore-based long-read sequencing before and after filtering. (**B**) Flow diagram of the genetic strategies for the proband. (**C**) Integrative genomics viewer (IGV) visualization of alignments of the Nanopore reads from the whole genome sequence analysis of the proband for chromosome 15

intron 8 of the canonical NM_002399.4 isoform of the *MEIS2* gene, and the downstream junction disrupted intron 2 of the canonical NM_022769.5 isoform of the CREB regulated transcription coactivator 3 (*CRTC3*) gene (Fig. 2C). The human *MEIS2* gene, located on chromosome 15q14, has been associated with intellectual disability, cleft palate, congenital heart defect, and facial dysmorphism at a variable severity (OMIM 600987) [7].

Figure 3A depicts a schematic representation of the inversion spanning 54 Mb on chromosome 15, and the predicted architecture of the paracentric inversion is shown in Fig. 3B. In order to confirm the inversion and its junctions at the single nucleotide level, specific primers were designed to amplify the junction sequences of the inverted allele, and the PCR products were analyzed by Sanger sequencing. As shown in Fig. 3C, Sanger

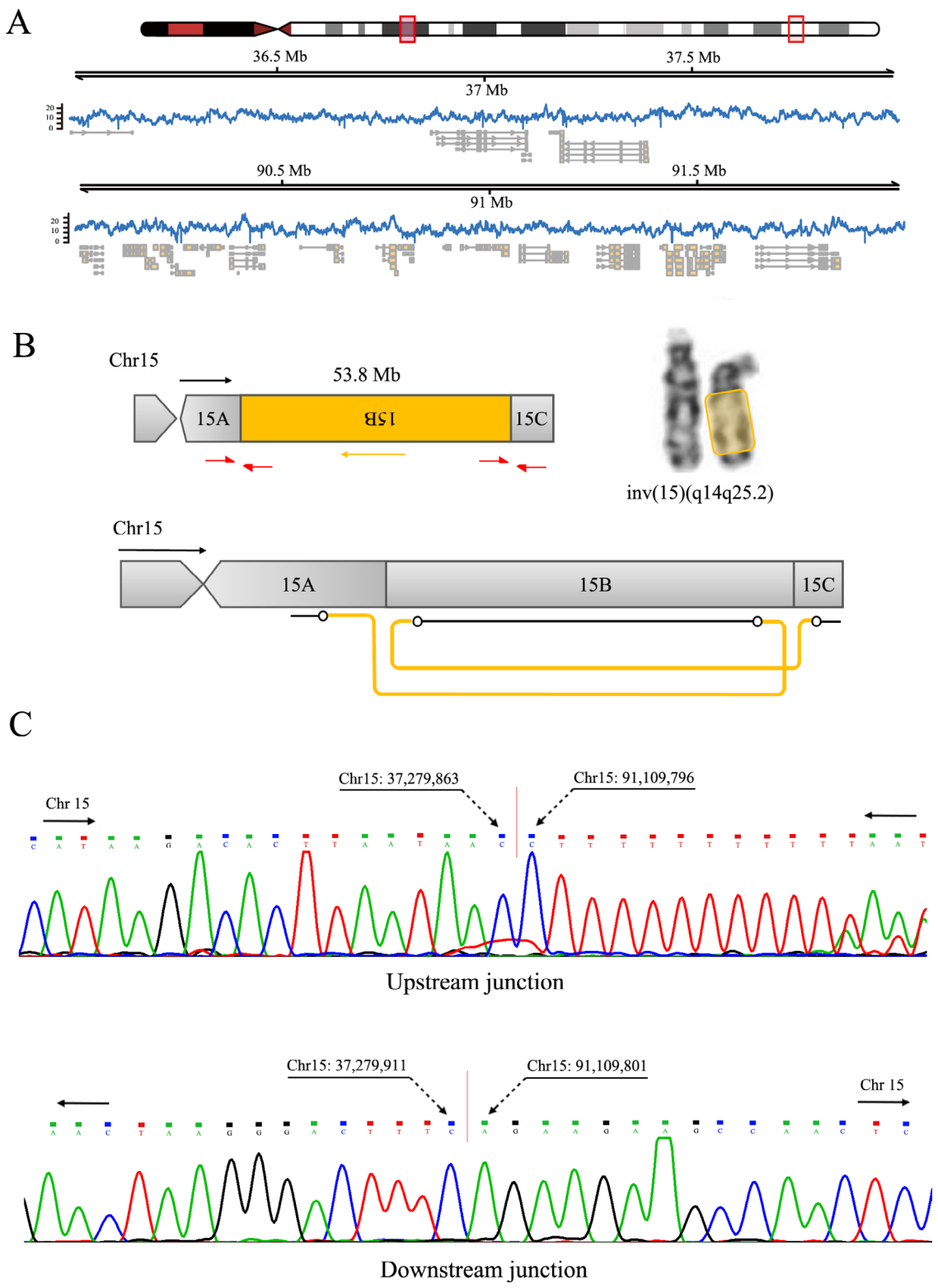

Fig. 3 Fine mapping of the paracentric inversion 46,XX, inv (15)(q15q26.1) by nanopore-based long-read sequencing. (**A**) Screenshot of the genomic regions containing 46,XX, inv (15)(q15q26.1). (**B**) The upper-left image indicates schematic representation for the paracentric inversion, in which a chromosomal segment is inverted in the opposite orientation. The red arrows denote the location of primers used for Sanger sequencing of breakpoints. The yellow arrow indicates the orientation of an un-inverted chromosome. In the upper-right image, the location of the paracentric inversion is highlighted in yellow. The below image denotes schematic diagram for the paracentric inversion. The black circles represent the breakpoints, and the yellow lines indicate the orientation of the paracentric inversion. (**C**) Sanger sequencing results for the PCR products including the breakpoints

sequencing confirmed the breakpoint junctions called by Sniffles. Meanwhile, PCR assays using specific primers targeting the inverted allele did not yield any products in either parent (data not shown), suggesting that this is a *de novo* inversion in the proband. Furthermore, sequence alignments revealed a 48-bp microdeletion in the *MEIS2* gene (upstream junction) and a 4-bp microdeletion in the *CRTC3* gene (downstream junction).

So far, a total of 11 mutations that truncate the MEIS2 protein have been reported in 14 patients [7–12]. The clinical phenotypes and mutations of these patients are presented in Table 1. The most commonly described clinical features in these reports were intellectual disability, cleft palate, and congenital heart defects. Other symptoms include delayed speech, psychomotor problems, autism, and fine arched eyebrows.

Discussion

Previous studies have identified several microdeletions, small insertions and deletions (indels), and SNVs in the *MEIS2* gene that cause intellectual disability, cleft palate, congenital heart defect, and facial dysmorphism at variable severity and penetrance [8, 13]. In this study, we reported a novel paracentric inversion disrupting the *MEIS2* gene. Because this is a large inversion greater than 57 Mb, the majority of conventional genetic analyses failed to identify the inversion. By using the long-read sequencing, we successfully detected, mapped, and characterized this unique inversion. Our strategies consist of G-banded karyotype analysis, chromosomal microarray analysis, whole exome sequencing, long-read sequencing, and Sanger sequencing, while long-read sequencing was proved powerful to detect new SVs that have not been identified by conventional genetic diagnosis methods.

Next generation sequencing (NGS) has been demonstrated to be powerful in uncovering causative pathogenic variants, thereby offering a cost-effective way for genetic diagnosis of monogenic diseases [14]. However, because of PCR-based and short-read sequencing tests, NGS is challenging to identify repeat expansion disorders, and SVs if the breakpoints are located in repetitive sequences [15]. In contrast, long-read sequencing not only accurately identifies SVs and provides orientation and sequencing information of SVs, but also achieves satisfying resolution in both exons and introns with repetitive sequences [16]. In the present study, on the basis of the accurate breakpoint information, we were able to design a PCR assay to precisely map the inversion in the proband. In clinical practice, the guideline recommends that patients with pediatric genetic diseases should receive routine genetic tests, including G-banded karyotype analysis, CMA and WES. However, we suggest that long-read sequencing should be directly used to identify atypical variants if routine approaches proved in vain.

Table 1 Clinical features for patients with mutations truncating MEIS2 protein

References	Verheije [7]								Hildebrand [9]	Santoro [8]		Su [10]	Giliberti [11]	Fujita [12]
Patients	1	2	3	4	5	6	7	8	9	10	11	12	13	14
Gender	M	M	M	F	M	F	F	F	F	M	M	M	M	F
Ages (years)	5	10	4	20	14	5	18	10	16	15	57	3	10	2
Ethnicity	Asian	Caucasian	Caucasian	Caucasian	Mexican	Caucasian	Asian - Caucasian	Caucasian	NA	NA	NA	Chinese	Caucasian	French
Mutation	c.978G > A (p.W326*)	c.639 + 1G > A	c.640–2 A > G	c.829 C > T (p.Q277*)	c.868dupA (p.I290Nfs*40)	c.978–2 A > G	c.383delA (p.K128Sfs*19)	c.934_937del (p.L312Rfs*11)	c.934_937delTTAG (p.L312Rfs*11)	c.27_28del (p.H10Lfs*84)	c.27_28del (p.H10Lfs*84)	c.998_1000delGAA (p.R333del)	c.520 C > T, p.R174*	c.611 C > G (p.S204*)
Cleft palate	+	+	+	+	+	+	-	+	+	+	-	-	-	+
Intellectual disability	+	+	+	+	-	+	-	-	NA	+	-	+	+	+
Congenital heart defects	+	NA	NA	+	-		+	+	NA	-	-	+	+	+
Proptosis	+	-	-	-	-	-	-	-	-	-	-	-	-	-
Psychomotor problems	+	+	NA	+	NA	-	+	-	-	-	-	-	NA	+
Small chin	+	-	-	-	-	-	-	-	-	-	-	-	-	-
Fine arched eyebrows	+	+	-	-	-	+	-	+	+	-	-	-	+	-
Delayed speech	+	+	+	+	-	+	-	+	+			+	+	+
Hearing loss	-	+	-	+	+	-	-	-	-			-	NA	NA
Autism	-	+	+	-	-	-	-	-	+	-	-	-	+	NA

M, male; +, present; -, absent; NA, not available. Reference sequence for *MEIS2* gene: NM_170674.4

MEIS2 encodes a homeodomain-containing transcription factor, which belongs to the highly conserved three amino acid loop extension (TALE) superfamily. Meis2 is widely expressed in multiple fetal tissues, including brain, hearts, forelimb buds and palatal shelves, and is critical for cranial and cardiac neural crest development [17]. Haploinsufficiency of the *MEIS2* gene has been shown to cause intellectual disability, cleft palate, congenital heart defect, and facial dysmorphism at variable severity and penetrance [7–9, 18]. Different mutation types in the *MEIS2* gene have been reported, including microdeletions, SNVs, and indels [13]. Generally, MEIS2 missense mutations are associated with more severe phenotypes than deletions, suggesting a possible dominant negative effect [19]. In this study, we reported for the first time a novel paracentric inversion completely disrupting the *MEIS2* gene, which can explain the phenotypes of the proband. It has been reported that palate defects occur in 80% (16/20) patients with MEIS2 mutations, and 85% (22/26) in cases with microdeletion and duplication [13]. Herein, our patient didn't have cleft palate, suggesting that a better definition of genotype-phenotype correlation could be possible if a greater number of patients with *MEIS2* mutations are available.

The expression analysis of *MEIS2* may be beneficial to clarify the correlation between genotype and phenotype. However, the expression of *MEIS2* could not be assessed in our patient because of highly degradation of RNA and proteins in archived blood samples. We have tried to re-recruit the proband, but the guardian of the proband refused test of intelligence scale for the proband and repeated blood draw. Thus, a limitation in our study is that the effects of the inversion on the expression of *MEIS2* are unknown.

Conclusions

In conclusion, we used long-read sequencing to identify and characterize a paracentric inversion that evaded detection by G-banded karyotype analysis, CMA, and WES. This inversion disrupted the *MEIS2* gene, and the clinical features of the proband were consistent with those of haploinsufficiency of the *MEIS2* gene. Taken together, long-read sequencing may possess significant value in elucidating the precise genetic etiology of patients with relatively nonspecific clinical findings and chromosomal inversion that are beyond the resolution of conventional approaches.

Author contributions

J.T., M.H., Z.X., and P.H. conceived and designed the study. J.T. and M.H. recruited the patients, contributed to clinical evaluations, performed long-read sequencing analysis. X.J. and A.L. performed G-banded karyotyping. F.Q. and C.Z. performed whole exome sequencing experiments and data analysis. L.M. and Y.W. performed chromosomal microarray and analysis. J.T. performed Sanger sequencing and wrote the first draft of the manuscript. Z.X., and P.H. revised the manuscript. All authors reviewed, commented, and agreed on the final draft of the manuscript.

Funding

This work was supported by the National Key R&D Program of China (No. 2022YFC2703400 and No. 2021YFC1005301), the National Natural Science Foundation of China (No. 81971398 and No. 82371862), and the Jiangsu Province Capability Improvement Project through Science, Technology and Education Jiangsu Provincial Medical Key Discipline (No. ZDXK202211).

Data availability

The sequencing data that support the findings of this study have been deposited into the European Variation Archive (EVA; https://www.ebi.ac.uk/eva/) with the accession number PRJEB79890.

Declarations

Ethics approval and consent to participate

The written informed consent for the study was obtained from the parents of the proband, and all procedures were reviewed and approved by the Institutional Review Board of Nanjing Women and Children's Healthcare Hospital (No. [2021] KY-104).

Consent for publication

The written informed consent for publication was obtained from the parents of the proband.

Clinical trial number

Not applicable.

Competing interests

The authors declare no competing interests.

Received: 23 August 2024 / Accepted: 21 November 2024
Published online: 09 January 2025

References

1. Kosuthova K, Solc R. Inversions on human chromosomes. Am J Med Genet A. 2023;191(3):672–83.
2. Schuy J, Grochowski CM, Carvalho CMB, Lindstrand A. Complex genomic rearrangements: an underestimated cause of rare diseases. Trends Genet. 2022;38(11):1134–46.
3. Rauch A, Ruschendorf F, Huang J, Trautmann U, Becker C, Thiel C, et al. Molecular karyotyping using an SNP array for genomewide genotyping. J Med Genet. 2004;41(12):916–22.
4. Lupski JR, Liu P, Stankiewicz P, Carvalho CMB, Posey JE. Clinical genomics and contextualizing genome variation in the diagnostic laboratory. Expert Rev Mol Diagn. 2020;20(10):995–1002.
5. Vicente-Salvador D, Puig M, Gaya-Vidal M, Pacheco S, Giner-Delgado C, Noguera I, et al. Detailed analysis of inversions predicted between two human genomes: errors, real polymorphisms, and their origin and population distribution. Hum Mol Genet. 2017;26(3):567–81.
6. Ebert P, Audano PA, Zhu Q, Rodriguez-Martin B, Porubsky D, Bonder MJ et al. Haplotype-resolved diverse human genomes and integrated analysis of structural variation. Science. 2021;372(6537).
7. Verheije R, Kupchik GS, Isidor B, Kroes HY, Lynch SA, Hawkes L, et al. Heterozygous loss-of-function variants of MEIS2 cause a triad of palatal defects, congenital heart defects, and intellectual disability. Eur J Hum Genet. 2019;27(2):278–90.
8. Santoro C, Riccio S, Palladino F, Aliberti F, Carotenuto M, Zanobio M, et al. A novel MEIS2 mutation explains the complex phenotype in a boy with a typical NF1 microdeletion syndrome. Eur J Med Genet. 2021;64(5):104190.
9. Hildebrand MS, Jackson VE, Scerri TS, Van Reyk O, Coleman M, Braden RO, et al. Severe childhood speech disorder: gene discovery highlights transcriptional dysregulation. Neurology. 2020;94(20):e2148–67.
10. Su JX, Velsher LS, Juusola J, Nezarati MM. MEIS2 sequence variant in a child with intellectual disability and cardiac defects: expansion of the phenotypic spectrum and documentation of low-level mosaicism in an unaffected parent. Am J Med Genet A. 2021;185(1):300–3.

11. Giliberti A, Currò A, Papa FT, Frullanti E, Ariani F, Coriolani G, et al. MEIS2 gene is responsible for intellectual disability, cardiac defects and a distinct facial phenotype. Eur J Med Genet. 2020;63(1):103627.
12. Fujita A, Isidor B, Piloquet H, Corre P, Okamoto N, Nakashima M, et al. De novo MEIS2 mutation causes syndromic developmental delay with persistent gastro-esophageal reflux. J Hum Genet. 2016;61(9):835–8.
13. Zhang B, Liu M, Fong CT, Iqbal MA. MEIS2 (15q14) gene deletions in siblings with mild developmental phenotypes and bifid uvula: documentation of mosaicism in an unaffected parent. Mol Cytogenet. 2021;14(1):58.
14. Sullivan JA, Schoch K, Spillmann RC, Shashi V. Exome/Genome sequencing in undiagnosed syndromes. Annu Rev Med. 2023;74:489–502.
15. Kumar KR, Cowley MJ, Davis RL. Next-generation sequencing and Emerging technologies. Semin Thromb Hemost. 2019;45(7):661–73.
16. Duan X, Pan M, Fan S. Comprehensive evaluation of structural variant genotyping methods based on long-read sequencing data. BMC Genomics. 2022;23(1):324.
17. Wang L, Tang Q, Xu J, Li H, Yang T, Li L, et al. The transcriptional regulator MEIS2 sets up the ground state for palatal osteogenesis in mice. J Biol Chem. 2020;295(16):5449–60.
18. Johansson S, Berland S, Gradek GA, Bongers E, de Leeuw N, Pfundt R, et al. Haploinsufficiency of MEIS2 is associated with orofacial clefting and learning disability. Am J Med Genet A. 2014;164A(7):1622–6.
19. Douglas G, Cho MT, Telegrafi A, Winter S, Carmichael J, Zackai EH, et al. De novo missense variants in MEIS2 recapitulate the microdeletion phenotype of cardiac and palate abnormalities, developmental delay, intellectual disability and dysmorphic features. Am J Med Genet A. 2018;176(9):1845–51.

Publisher's note